Separation Science and Technology
Publication details, including instructions for authors and subscription information:
http://www.informaworld.com/smpp/title~content=t713708471

Energy Consumption and Its Reduction in the Hydrocyclone Separation Process. II. Time-Averaged and Fluctuating Characteristics of the Turbulent Pressure in a Hydrocyclone

Liang-Yin Chu[ab]; Jian-Jun Qin[b]; Wen-Mei Chen[b]; Xiao-Zhong Lee[b]
[a] Nakao Laboratory, Department of Chemical System Engineering, School of Engineering, The University of Tokyo, Tokyo, Japan [b] SCHOOL OF CHEMICAL ENGINEERING, SICHUAN UNIVERSITY, CHENGDU, SICHUAN, CHINA

Online publication date: 27 November 2000

To cite this Article Chu, Liang-Yin , Qin, Jian-Jun , Chen, Wen-Mei and Lee, Xiao-Zhong(2000) 'Energy Consumption and Its Reduction in the Hydrocyclone Separation Process. II. Time-Averaged and Fluctuating Characteristics of the Turbulent Pressure in a Hydrocyclone', Separation Science and Technology, 35: 15, 2543 — 2560
To link to this Article: DOI: 10.1081/SS-100102355
URL: http://dx.doi.org/10.1081/SS-100102355

SEPARATION SCIENCE AND TECHNOLOGY, **35**(15), pp. 2543–2560, 2000

Energy Consumption and Its Reduction in the Hydrocyclone Separation Process. II. Time-Averaged and Fluctuating Characteristics of the Turbulent Pressure in a Hydrocyclone

LIANG-YIN CHU,* JIAN-JUN QIN, WEN-MEI CHEN, and XIAO-ZHONG LEE
SCHOOL OF CHEMICAL ENGINEERING
SICHUAN UNIVERSITY
CHENGDU, SICHUAN 610065, CHINA

ABSTRACT

A resistance wire strain gauge system was used to experimentally study time-averaged and fluctuating characteristics of turbulent pressure in a hydrocyclone for the first time. In the main space inside the hydrocyclone, pressure distribution could be described with a mathematical model in which pressure is a function of positional radius. When positional radius decreases, pressure drops, but the radial gradient of pressure increases. In the central area under the vortex finder, the radial gradient of pressure, pressure fluctuation, and relative pressure fluctuation are all very large. That is, both energy loss and turbulent energy dissipation are serious in this area. In the main space inside the hydrocyclone, turbulent pressure mostly fits in Gaussian distribution. At some positions within the cylindrical area and the upper part of inner helical flow, turbulent pressure does not fit in Gaussian distribution, which indicates turbulent fine-structure intermittency exists at these positions in the hydrocyclone.

Key Words. Hydrocyclone; Turbulence; Energy consumption; Energy saving; Pressure distribution; Time-averaged characteristics; Fluctuating characteristics

* To whom correspondence should be addressed. Before September 2001: Nakao Laboratory, Department of Chemical System Engineering, School of Engineering, The University of Tokyo, 7-3-1 Hongo, Bunkyo-ku, Tokyo 113-8656, Japan. E-mail chu@nakao1.t.u-toyko.ac.jp

INTRODUCTION

Hydrocyclone separation is becoming a universal separation technique. There have been numerous successful applications of this separation technique in many industries, such as mineral processing, petrochemical engineering, chemical engineering, and environmental engineering. More and more attention is being paid to hydrocyclones. Unfortunately, one of the main disadvantages in conventional hydrocyclone separations is that energy consumption is high, resulting in high operating costs. To make good use of energy and reduce the operating costs of hydrocyclone separation, it is essential to investigate the energy-consumption mechanism and energy-saving principles.

Energy consumption in a hydrocyclone is dependent on the turbulent pressure inside the hydrocyclone to a considerable degree. Therefore, it is essential to investigate the pressure field to understand the energy-consumption mechanism. Unfortunately, there have not been any systematical experimental investigations of the structure of turbulent pressure in hydrocyclones. Previous experimental research on turbulent flow fields in hydrocyclones focused on flow pattern and velocity field; only a few considered pressure characteristics, even though the pressure structure is also important for understanding the separation process in hydrocyclones. The fluctuating phenomenon is one of the most important characteristics of turbulent structures. However, previous investigations on pressure characteristics only gave time-averaged pressures at some partial positions in hydrocyclones, because it is difficult to measure the fluctuating characteristics of turbulent pressure, because of the limitation of measurement instruments. For flow pattern and velocity field, the measurement instrument could be a non-contact-type instrument, e.g., tracer (1), dyeing (2, 3), or Laser Doppler Anemometer (4, 5). The measurement of pressure has had to depend on contact-type instruments up to now. A pilot gauge with usual dimensions could not be used to measure pressure fluctuation because the resulting inertia is too large (6).

For the first time, a resistance wire strain gauge system was used to experimentally investigate both the time-averaged and fluctuating characteristics of turbulent pressure in hydrocyclones.

EXPERIMENTAL

Instrument and Apparatus

When a turbulent flow field is measured with a contact-type instrument, examining elements and related instruments must meet a series of demands (6). After considering these demands, syringe needles with an outer diameter of 1.4 mm and an inner diameter of 0.8 mm were selected as pressure probes. Tests confirmed that the selected syringe needles had enough strength and rigidity to measure pressure inside hydrocyclones. A BPR-12-type of resis-

tance wire strain gauge, with rated pressure of 0.1 MPa, was chosen as a pressure sensor. Nonlinear error, delay error, and duplication error of the gauge were all less than 0.2%. The magnitude of output voltage signal from the pressure sensor was in millivolts, thus the signal should be amplified before being sent to a data-collection system. The signal transmission line was shielded to prevent interferential signals from infiltrating. The automatic on-line data-collection system with synchronous treatment was mainly composed of a HT-1232-type of A/D converter, a digital signal display, a computer, and relevant software. The A/D conversion was triggered by software, with a typical time of 10 μs, converting precision of ±0.03%, and nonlinear error of ±1 LSB. The static-pressure test of this pressure-measurement system showed that both overall nonlinear error and range error were less than 0.25%.

The schematic diagram of the experimental system is shown in Fig. 1. The system was composed of a hydrocyclone, liquid-transportation system, and pressure-measurement system.

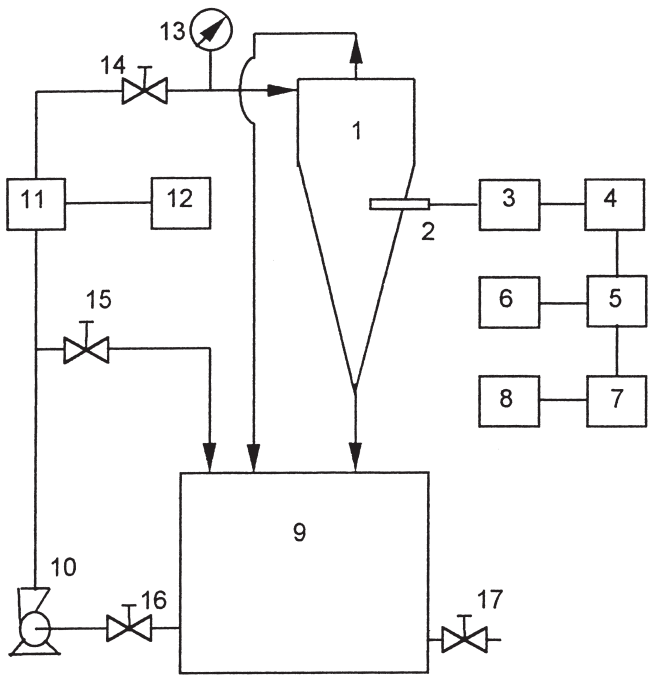

FIG. 1 Schematic diagram of the experimental system: (1) hydrocyclone; (2) pressure probe; (3) pressure sensor; (4) amplifier; (5) A/D converter; (6) digital display; (7) computer; (8) printer; (9) water tank; (10) pump; (11) electromagnetic flowmeter; (12) digital display; (13) gauge; (14)–(17) valves.

The geometry of the hydrocyclone used in the experiments is shown in Fig. 2. The hydrocyclone was made up of an overflow volute, inlet, vortex finder, cylindrical section, cone section, underflow pipe, and underflow transit box. The geometry of the hydrocyclone was designed according to Rietema's optimum geometry for separation (7). The ratio of the length of the cylindrical part to the hydrocyclone diameter was 1.6, and the value of H in Fig. 2 was 120 mm.

Program

The liquid used in the experiments was water. The measured points for pressure inside the hydrocyclone were distributed as shown in Fig. 3. At those

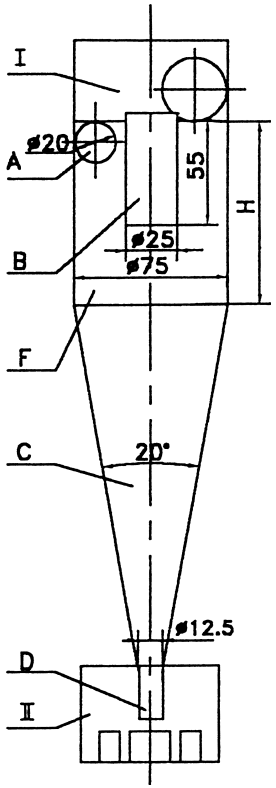

FIG. 2 Hydrocyclone geometry: (A) inlet; (B) vortex finder; (C) cone section; (D) underflow pipe; (F) cylindrical section; (I) overflow volute; (II) underflow transit box.

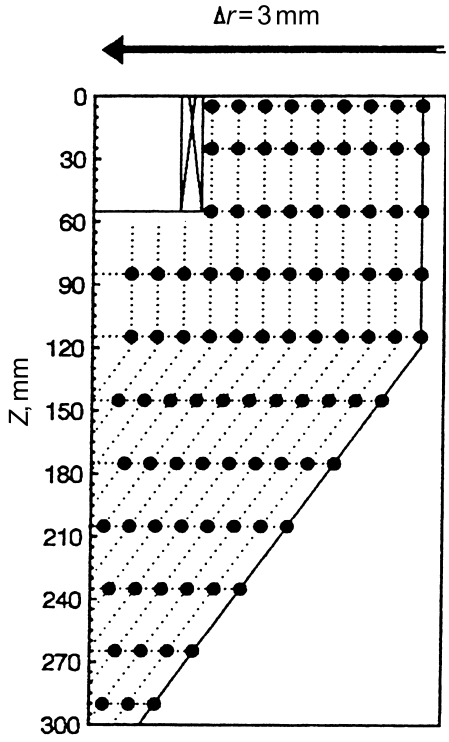

FIG. 3 Distribution of measured points in the hydrocyclone.

axial positions with axial distance from the top (Z) being 5, 25, 55, 85, 115, 145, 175, 205, 235, 265, and 290 mm, measurement holes were made in the hydrocyclone wall, and every hole was sealed by elastic rubber. A pressure probe could be inserted radially into the hydrocyclone by passing through the elastic rubber. The radial step of the measured points in the hydrocyclone was 3 mm. Thus, the measured points in the hydrocyclone were a series of netted points. Because the flow fields in hydrocyclones could be taken as axially symmetrical fields (8), it is enough to understand the pressure structure in hydrocyclones by measuring the pressure at those points, as illustrated in Fig. 3.

To investigate the pressure distribution at the entrance of hydrocyclone, pressure probes were also set around the inlet with the same method as mentioned above. These measured points were all set in the same horizontal level as that of the inlet axis. The distance between two adjacent measured points in inlet wall was 20 mm, and points in the hydrocyclone wall were arranged with the central angle between two adjacent points as 30°.

Constant inlet pressure of 0.08 MPa was maintained. The capacity of the hydrocyclone was measured by an electromagnetic flow meter.

RESULTS AND DISCUSSION

Time-Averaged Characteristics of Turbulent Pressure

Radial Distribution of Pressure in the Hydrocyclone

Radial distribution of pressure in the hydrocyclone is shown in Fig. 4. Experimental radial distribution of pressure fits well with theoretical results (9). With positional radius decreasing, pressure drops; meanwhile, the radial gradient of the pressure increases. An exceptional phenomenon was found: the radial drop of pressure is very small in the annular space between the outer wall of vortex finder and the inner wall of hydrocyclone, and pressure even rises slightly near the outer wall of the vortex finder.

In a sense, the overall pressure of liquid stands for usable mechanical energy (10). The overall pressure drop could be used to characterize energy loss.

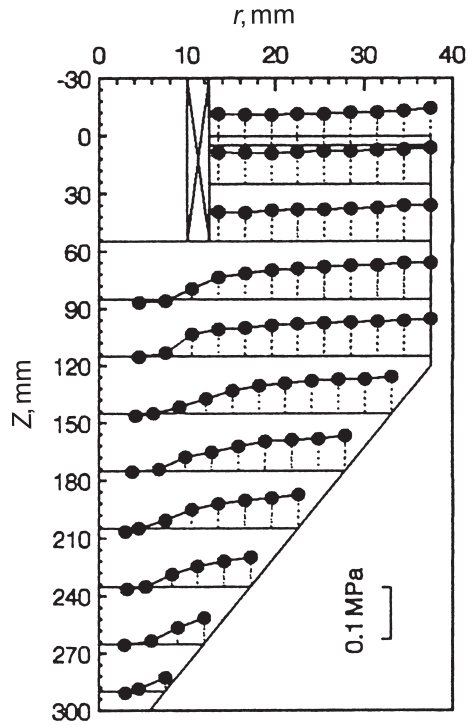

FIG. 4 Radial distribution of pressure in the hydrocyclone.

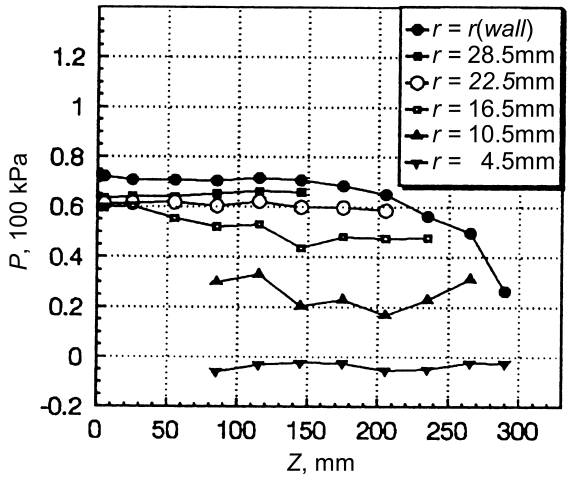

FIG. 5 Axial distribution of pressure in the hydrocyclone.

Therefore, energy loss in the annular space between the vortex finder wall and the hydrocyclone wall is small, but it is serious in the inner helical flow below the vortex finder. Most of the energy loss in the hydrocyclone is distributed in the central space below the vortex finder. Consequently, controlling the structure of the flow field in the central area near the hydrocyclone axis could be an effective way to reduce energy loss inside hydrocyclones.

Axial Distribution of Pressure in the Hydrocyclone

Figure 5 shows the experimental axial distribution of pressure in the hydrocyclone, where $r(wall)$ stands for the radius of the inner surface of hydrocyclone wall at a certain axial position. The curve of $r = r(wall)$ illustrates the axial distribution of pressure on the inner surface of hydrocyclone wall. Pressure barely drops axially near the hydrocyclone wall in the cylindrical section, but decreases sharply with increasing axial distance in the cone section. When the radial position is fixed, pressure varies little with the variation of axial position.

Time-Averaged Characteristics of a Pressure Field

A three-dimensional surface plot for a time-averaged pressure field in the hydrocyclone is shown in Fig. 6. The central area in the inner helical flow under the vortex finder is a space where pressure decreases sharply; while in the other areas inside the hydrocyclone, pressure drop is minimal.

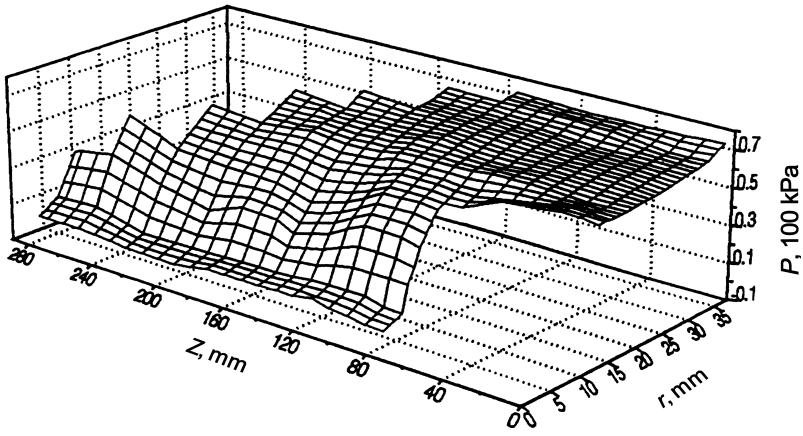

FIG. 6 Three-dimensional surface plot for the time-averaged pressure field in the hydrocyclone.

Figure 7 is a contour plot for a time-averaged pressure field in the hydrocyclone. Contour lines of pressure in the hydrocyclone are almost all parallel to the hydrocyclone axis. Where contour lines are denser, the pressure gradient is larger, i.e., pressure loss is larger, and therefore energy loss is more serious. Figure 7 shows that the area where energy loss is significant is the annular space between radii $r = 0.14R$ and $r = 0.45R$, where r is the positional radius, and R is the radius of the hydrocyclone.

Except those positions near the outer wall of the vortex finder, radial distribution curves of pressure in the hydrocyclone are almost all coincident. There-

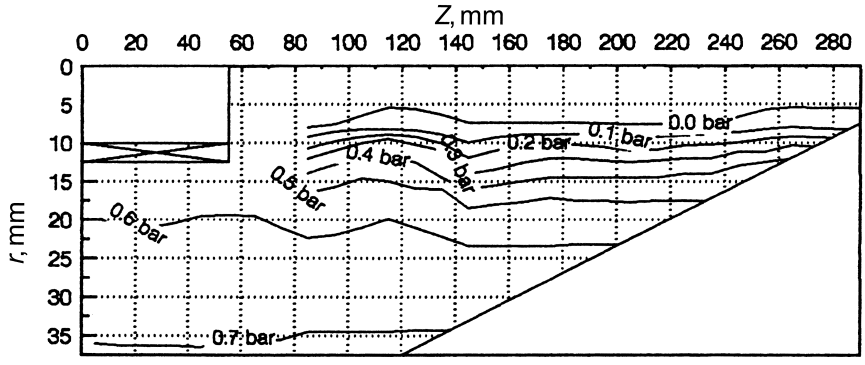

FIG. 7 Contour plot for the time-averaged pressure field in the hydrocyclone.

fore, the relationship between positional radius and pressure in the hydrocyclone could be described with the following mathematical model

$$P = 70 - 72.5 \exp[-0.06[r - 4.5)^{1.22}], \qquad (r \geq 4.5\text{mm}) \qquad (1)$$

Where, P (kPa) is the pressure of liquid at the radial position with a radius of r (mm).

Pressure Distribution at the Entrance of the Hydrocyclone

Experimental pressure distribution at the entrance of the hydrocyclone is shown in Fig. 8. At those points near the entrance of the hydrocyclone, pressures are almost at the same pressure level. Although the pressure varies slightly at one or two points, the variation is much smaller than that in the main space inside the hydrocyclone. That is to say, when the movement of fluid flow is changed from a one-dimensional rectilinear motion into a three-dimensional cyclonic motion at the entrance of the hydrocyclone, the pressure is barely reduced. This indicates that energy loss is not as serious as imagined at the entrance of the hydrocyclone. Compared with energy loss in the central space inside the hydrocyclone, energy loss at the entrance could even be neglected.

Fluctuating Characteristics of Turbulent Pressure

Pressure Fluctuation and Relative Pressure Fluctuation

Fluctuation phenomenon is an important characteristic of turbulent structures. In a turbulent flow field, turbulent pressure could be taken as the sum of

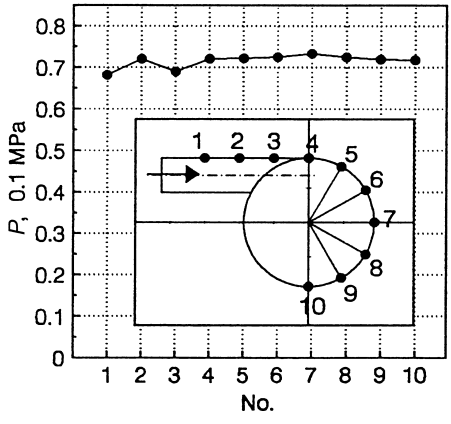

FIG. 8 Pressure variation at the entrance of hydrocyclone.

time-averaged pressure and fluctuating pressure. To characterize the intensity of pressure fluctuation, the concept of mean-square deviation of the least-square method is introduced. The larger the mean-square deviation of turbulent pressure, the more serious the pressure fluctuation phenomenon is. Two characteristic parameters are

a. Pressure fluctuation: the mean-square deviation of turbulent pressure, i.e.,

$$PF = \delta_P \tag{2}$$

where, PF is pressure fluctuation, and δ_P is the mean-square deviation of turbulent pressure, and

b. Relative pressure fluctuation: the ratio of the mean-square deviation of turbulent pressure to the time-averaged pressure, i.e.,

$$RPF = \frac{PF}{P} = \frac{\delta_P}{P} \tag{3}$$

where, RPF is relative pressure fluctuation and P is time-averaged pressure.

The energy needed for maintaining turbulence is taken from the averaged motion and then transferred to the turbulent motion (6). Therefore, the pressure fluctuation could be used to characterize the absolute value of energy taken from the averaged motion, and the relative pressure fluctuation could be adopted to characterize the ratio of energy taken from averaged motion to the total energy in averaged motion.

Pressure Fluctuation in the Hydrocyclone. Radial distribution of pressure fluctuation in the hydrocyclone is illustrated in Fig. 9. Pressure fluctuations are within 0.5–0.6 kPa inside the hydrocyclone. With positional radius decreasing, pressure fluctuation first reduces near the hydrocyclone wall, then enters a relatively steady area, and finally increases sharply in the central space near the air core. This radial-distribution law of pressure fluctuation is the same as that of velocity turbulence in hydrocyclones, which has been measured by Laser Doppler Velocimeter (LDV) (11). This consistency indicates the pressure-measurement-instrument system used in this investigation is appropriate for studying turbulent pressure.

Both pressure fluctuation and velocity turbulence are very large in the inner helical flow area near the air core inside the hydrocyclone; that is, both the energy taken from averaged motion by turbulent motion and the energy dissipated in turbulent motion are serious in this area. Therefore, controlling the structure of turbulent flow in the inner helical flow area near the air core should be the key to reducing energy loss in hydrocyclones.

Because of both the pressure of the helical flow on the hydrocyclone wall and the friction between the helical flow and the hydrocyclone wall, pressure

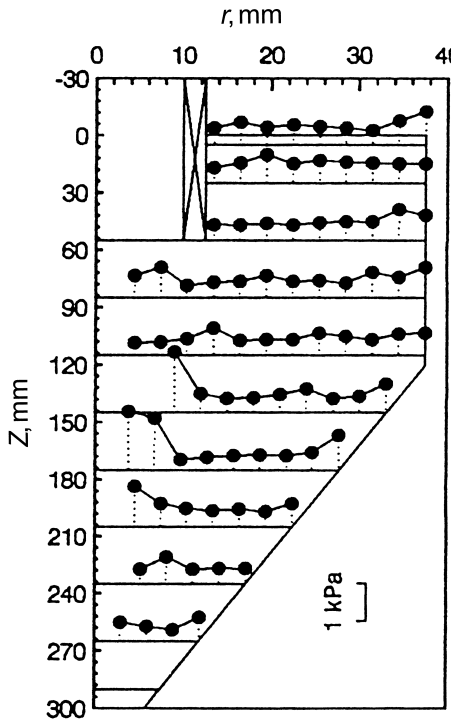

FIG. 9 Radial distribution of pressure fluctuation in the hydrocyclone.

fluctuation is large near the hydrocyclone wall. Turbulence is so violent in the inner helical flow near the air core because all the shape, size, and space positions of the air core are very unsteady, and the fluid around the air core is forced to rock with the air core. Therefore, the fluid flow should be in a turbulent state. Additionally, the large radial pressure gradient and large radial velocity gradient in the inner helical flow around the air core indicate that transformation between the pressure head and the kinetic head in this area is intensive, which contributes to the turbulence. Improving the existing state of the air core and the flow structure of fluid around the air core should effectively reduce energy loss in hydrocyclones.

Relative Pressure Fluctuation in the Hydrocyclone. Figure 10 shows radial distribution of relative pressure fluctuation in the hydrocyclone. In the area where the positional radius is larger than the outer radius of the vortex finder, relative pressure fluctuations are steady within 0.6–1.0%. This indicates that energy taken from averaged motion by turbulent motion is low in this area and only accounts for 0.6–1.0% of total energy in averaged motion.

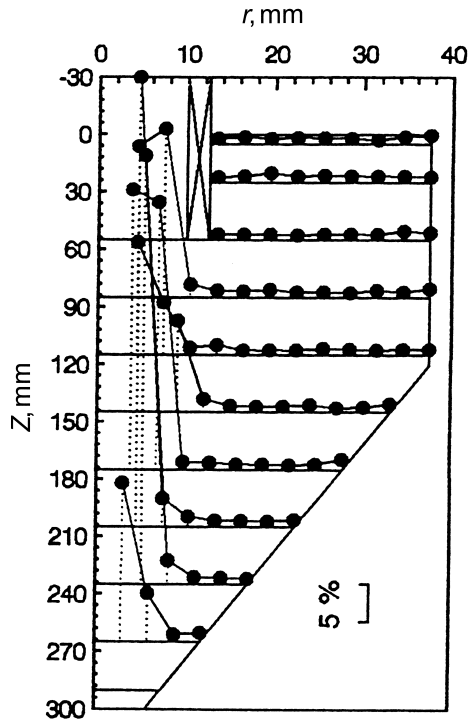

FIG. 10 Radial distribution of relative pressure fluctuation in the hydrocyclone.

However, in the space where the positional radius is smaller than the outer radius of the vortex finder, relative pressure fluctuation increases sharply with decreasing radius and the gradient is very large in the upper central area of the cone section. This again shows that the violent turbulent motion in the inner helical flow under the vortex finder results in considerable energy consumption. The ratio of the energy taken from averaged motion to the total energy in averaged motion is as high as 60% at one or two points. Controlling the structure of turbulence in the inner helical flow under the vortex finder should be considered for reducing energy loss in hydrocyclones.

Pressure Fluctuation and Relative Pressure Fluctuation at the Entrance of the Hydrocyclone. Pressure fluctuation and relative pressure fluctuation at the entrance of the hydrocyclone are shown in Fig. 11. When fluid flows from test points 1 to 10, the variation law of pressure fluctuation is similar to that of relative pressure fluctuation, because the time-averaged pressure varies little in this flow region. From test points 1 to 6, both pressure fluctuation and relative pressure fluctuation increase slightly, then

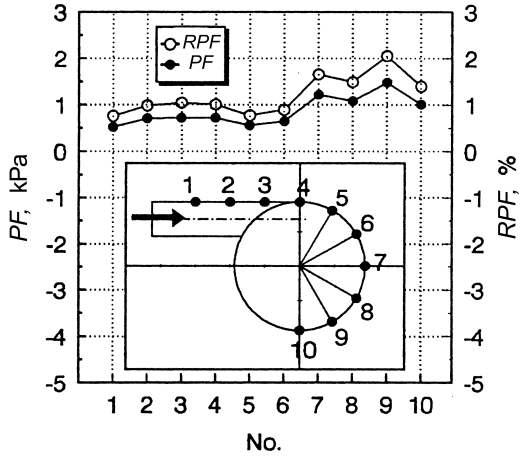

FIG. 11 Pressure fluctuation and relative pressure fluctuation at the entrance of hydrocyclone.

decrease slightly. Both the sudden enlargement of the cross-sectional area of fluid flow and the orientation variation of fluid flow will contribute to turbulence near the entrance. From test points 6 to 10, both pressure fluctuation and relative pressure fluctuation increase quite notably, which indicates that violent helical flow in hydrocyclones causes larger pressure fluctuation near the wall rather than in the pipe flow at the inlet. Compared with fluctuation in the main space inside the hydrocyclone, turbulence is less than expected at the entrance of the hydrocyclone.

Distribution Characteristics of the Probability Density of Turbulent Pressure

Besides pressure fluctuation and relative pressure fluctuation, distribution characteristics of probability density of turbulent pressure are also important for describing the fluctuating structure of a pressure field. To quantitatively describe the deviation of probability distribution of turbulent pressure from Gaussian distribution, two coefficients are introduced (12)

a. Skewness coefficient

$$B_S = \frac{\mu_3}{\sigma^3} \tag{4}$$

where, B_S is the skewness coefficient for describing skewness of a distribution, μ_3 is a three-order central matrix, and σ is the standard deviation.

TABLE 1
Skewness Coefficient (B_s), Kurtosis Coefficient (B_k), and Gaussian Distribution (G.D.) Test of Turbulent Pressure in the Hydrocyclone

		Z, mm										
r, mm		5	25	55	85	115	145	175	205	235	265	290
37.5	B_s	0.951	0.100	−0.006	1.401	0.091						
	B_k	4.334	2.909	2.258	5.698	2.368						
	G.D.	No	Yes	Yes	No	Yes						
34.5	B_s	0.350	0.199	−0.300	−0.183	−0.129	0.524					
	B_k	2.298	2.757	2.496	2.473	2.284	2.392					
	G.D.	Yes	Yes	Yes	Yes	Yes	Yes					
31.5	B_s	0.113	0.148	−0.356	0.048	0.133	0.152					
	B_k	2.679	2.408	2.679	3.432	2.540	2.532					
	G.D.	Yes	Yes	Yes	Yes	Yes	Yes					
28.5	B_s	−0.165		−0.038	0.032	0.033	−0.101	1.266				
	B_k	2.942		2.413	2.254	2.643	2.609	4.966				
	G.D.	Yes		Yes	Yes	Yes	Yes	No				
25.5	B_s	−0.041	0.268	0.053	0.143	0.179	0.128	−0.256	0.347			
	B_k	2.798	3.078	2.543	2.205	2.139	2.315	2.428	2.233			
	G.D.	Yes	Yes	Yes	Yes	Yes	Yes	Yes	Yes			
22.5	B_s	0.144	−0.199	−0.799	−0.113	0.117	−0.185	−0.003	0.111			
	B_k	2.810	2.498	4.789	2.515	2.600	2.384	2.430	2.332			
	G.D.	Yes	Yes	No	Yes	Yes	Yes	Yes	Yes			

19.5	B_s	0.077	1.036	0.329	−0.500	0.225	−0.064	0.129	0.254	0.019		
	B_k	2.500	3.643	2.877	2.813	2.774	3.118	2.849	2.412	2.464		
	G.D.	Yes	No	Yes	Yes	Yes	Yes	Yes	Yes	Yes		
16.5	B_s	−0.344	0.380	−0.066	−0.112	−0.181	−0.223	0.089	−0.229	0.215	−0.151	
	B_k	2.526	2.496	2.575	2.731	2.712	2.483	2.231	2.381	2.576	2.381	
	G.D.	Yes	Yes	Yes	Yes	Yes	Yes	Yes	Yes	Yes	Yes	
13.5	B_s	0.267	0.409	0.090	−0.074	−0.329	−0.777	0.194	0.051	0.075	−0.018	
	B_k	2.509	2.670	2.467	2.735	2.151	2.865	2.278	3.136	2.546	2.460	
	G.D.	Yes	Yes	Yes	Yes	Yes	No	Yes	Yes	Yes	Yes	
10.5	B_s				0.019	0.392	1.007	−0.648	−0.822	−0.052	−0.473	
	B_k				2.217	2.796	2.673	2.271	2.800	2.622	3.122	
	G.D.				Yes	Yes	No	No	No	Yes	Yes	
7.5	B_s				−0.238	−0.149		0.152	−0.327	−0.475	0.241	−0.009
	B_k				2.426	2.582		1.847	1.902	2.755	2.458	2.042
	G.D.				Yes	Yes		No	No	Yes	Yes	Yes
4.5	B_s				−0.769	0.198			0.064	0.045	−0.419	
	B_k				4.001	2.758			2.857	1.899	2.711	
	G.D.				No	Yes			Yes	No	Yes	

b. Kurtosis coefficient

$$B_K = \frac{\mu_4}{\sigma^4} \tag{5}$$

where, B_K is the kurtosis coefficient for describing kurtosis of a distribution, and μ_4 is a four-order central matrix.

When the sample number is large enough, skewness coefficient and kurtosis coefficient could be calculated by the following formulas

$$B_S = \frac{\sqrt{n}\,\Sigma(X_i - \overline{X})^3}{[\Sigma(X_i - \overline{X})^2]^{3/2}} \tag{6}$$

and

$$B_K = \frac{n\,\Sigma(X_i - \overline{X})^4}{[\Sigma(X_i - \overline{X})^2]^2} \tag{7}$$

where, n is the sample number, X_i is the individual sample value, and $\overline{X}$ is the averaged value of the overall samples.

For Gaussian distribution, the skewness coefficient is equal to zero, and the kurtosis coefficient is equal to three. Therefore, the skewness coefficient and the kurtosis coefficient could be introduced to jointly test and describe the deviation of the probability distribution of turbulent pressure from Gaussian distribution.

Experimental skewness coefficient, kurtosis coefficient, and Gaussian distribution test of turbulent pressure inside the hydrocyclone and at the entrance of the hydrocyclone are shown in Tables 1 and 2, respectively, where the symbol "Yes" stands for turbulent pressure that fits in Gaussian distribution and "No" for the contrary. A Gaussian distribution test was carried out according to a skewness coefficient in combination with a kurtosis coefficient. Figure 12 illustrates the Gaussian distribution test at the level of $\alpha = 0.05$ and $\alpha = 0.01$, where turbulent pressure was taken as fitting in Gaussian distribution if point $(|B_S|, B_k)$ falls into the range enclosed by the critical lines, and vice versa.

TABLE 2
Skewness Coefficient (B_s), Kurtosis Coefficient (B_k) and Gaussian Distribution (G.D.) Test of Turbulent Pressure at the Entrance of Hydrocyclone

No.	1	2	3	4	5	6	7	8	9	10
B_s	0.348	0.211	0.080	0.148	0.091	0.005	0.072	0.114	0.186	0.010
B_k	3.252	2.276	2.368	2.544	2.735	2.091	2.113	2.212	2.225	2.748
G.D.	Yes	Yes	Yes	Yes	Yes	Yes	Yes	Yes	Yes	Yes

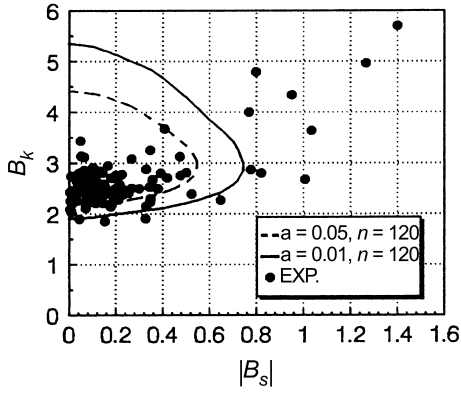

FIG. 12 Gauss distribution test of the turbulent pressure inside hydrocyclone and at the entrance of hydrocyclone.

Figure 12 shows that turbulent pressures fit in Gaussian distribution at most positions inside the hydrocyclone and at the entrance of the hydrocyclone. The Gaussian distribution tests in Tables 1 and 2 were carried out at $\alpha = 0.01$.

Table 1 shows turbulent pressures mostly fit in Gaussian distribution inside the hydrocyclone; while at some positions in cylindrical space and in the upper inner helical flow region, turbulent pressures do not fit in Gaussian distribution. These non-Gaussian distributions indicate that turbulent fine-structure intermittency (13, 14) exists at these positions. In Table 2, all turbulent pressures fit in Gaussian distribution at the entrance of the hydrocyclone.

CONCLUSIONS

1. With positional radius decreasing, time-averaged pressure drops, whereas radial pressure gradient increases. In the main space inside hydrocyclones, time-averaged pressure barely varies with the variation of axial positions, but varies with positional radius. The contour lines of pressure are almost all parallel to the hydrocyclone axis. Pressure distribution could be described with a mathematical model in which pressure is a function of positional radius in the hydrocyclone.

2. In the inner helical flow under the vortex finder, the radial pressure gradient, pressure fluctuation, and relative pressure fluctuation are all very large. That is, energy loss and turbulent energy dissipation are serious in this area. At the entrance of the hydrocyclone, the pressure drop, pressure fluctuation, and relative pressure fluctuation are not significant. Both energy loss and turbulent energy dissipation are not as serious at the entrance as expected.

3. Turbulent pressures inside the hydrocyclone mostly fit in Gaussian distribution, but at some positions in the cylindrical area and the upper inner helical flow area turbulent pressure does not fit in Gaussian distribution, which indicates that turbulent fine-structure intermittency exists at these positions.

ACKNOWLEDGEMENTS

This research was supported by the China Postdoctoral Science Foundation and the Doctoral Science Foundation of the State Education Ministry of China.

REFERENCES

1. D. F. Kelsall, "A study of the motion of solid particles in a hydraulic cyclone," *Trans. Inst. Chem. Eng., 30,* 87–108 (1952).
2. P. Bhattacharyya, "The flow field inside a conventional hydrocyclone," in *Proc. 2nd Int. Conf. on Hydrocyclones,* Bath, UK, 323–334, Sept. 1984.
3. D. Bradley and D. J. Pulling, "Flow patterns in the hydraulic cyclone and their interpretation in terms of performance," *Trans. Inst. Chem. Eng., 37,* 34–45, 1959.
4. J. Xu, Q. Luo, and J. Qiu, "Studying the flow field in a hydrocyclone with no forced vortex. I. Time-averaged velocity," *Filtr. Separ., 7/8,* 276–278 (1990).
5. L.-Y. Chu and W.-M. Chen, "Research on the motion of solid particles in the hydrocyclone." *Sep. Sci. Technol., 28*(10), 1875–1886, 1993.
6. J. O. Hinze, *Turbulence* (2d ed.), McGraw-Hill, New York, 1979.
7. K. Rietema, "Performance and design of hydrocyclones. IV. Design of hydrocyclones," *Chem. Eng. Sci., 15*(3/4), 320–325 (1961).
8. L. Svarovsky, *Hydrocyclones,* Holt, Rinehart and Winston, Eastbourne, UK, 1984.
9. L.-Y. Chu, X.-Z. Lee, and W.-M. Chen, "Energy consumption and its reduction in hydrocyclone separation process. I. Theoretical investigations of pressure distribution and energy consumption mechanism in hydrocyclones," in *Proc. 7th World Filtration Congress, Budapest, Hungary,* Vol. I, 152–156, May 1996.
10. I. H. Shames, *Mechanics of Fluids* (2d ed.), McGraw-Hill, New York, 1981.
11. J. Xu, Q. Luo, and J. Qiu, "Studying the flow field in a hydrocyclone with no forced vortex. II. Turbulence," *Filtr. Separ. 9/10,* 356–359 (1990).
12. M. Abramowitz, and I. A. Steyun, eds., *Handbook of Mathematical Functions.* Dover, New York, 1972, p. 928.
13. G. K. Batchelor, and A. A. Townsend, "The nature of turbulent motion at large wave-numbers," *Proc. Roy. Soc. A, 199,* 238, 1949.
14. W. D. McComb, *The Physics of Fluid Turbulence,* Clarendon Press, Oxford, 1990.

Received by editor November 9, 1999
Revision received April 2000